Published OnlineFirst September 18, 2019; DOI: 10.1158/1078-0432.CCR-19-0799

Clinical Cancer Research

Glycogen Synthase Kinase-3 Inhibition Sensitizes Pancreatic Cancer Cells to Chemotherapy by Abrogating the TopBP1/ATR-Mediated DNA Damage Response

Li Ding[1], Vijay S. Madamsetty[2], Spencer Kiers[1], Olga Alekhina[1], Andrey Ugolkov[3], John Dube[1], Yu Zhang[1], Jin-San Zhang[1,4], Enfeng Wang[2], Shamit K. Dutta[2], Daniel M. Schmitt[3], Francis J. Giles[3], Alan P. Kozikowski[5], Andrew P. Mazar[6], Debabrata Mukhopadhyay[2], and Daniel D. Billadeau[1]

Abstract

Purpose: Pancreatic ductal adenocarcinoma (PDAC) is a predominantly fatal common malignancy with inadequate treatment options. Glycogen synthase kinase 3β (GSK-3β) is an emerging target in human malignancies including PDAC.

Experimental Design: Pancreatic cancer cell lines and patient-derived xenografts were treated with a novel GSK-3 inhibitor 9-ING-41 alone or in combination with chemotherapy. Activation of the DNA damage response pathway and S-phase arrest induced by gemcitabine were assessed in pancreatic tumor cells with pharmacologic inhibition or siRNA depletion of GSK-3 kinases by immunoblotting, flow cytometry, and immunofluorescence.

Results: 9-ING-41 treatment significantly increased pancreatic tumor cell killing when combined with chemotherapy. Inhibition of GSK-3 by 9-ING-41 prevented gemcitabine-induced S-phase arrest suggesting an impact on the ATR-mediated DNA damage response. Both 9-ING-41 and siRNA depletion of GSK-3 kinases impaired the activation of ATR leading to the phosphorylation and activation of Chk1. Mechanistically, depletion or knockdown of GSK-3 kinases resulted in the degradation of the ATR-interacting protein TopBP1, thus limiting the activation of ATR in response to single-strand DNA damage.

Conclusions: These data identify a previously unknown role for GSK-3 kinases in the regulation of the TopBP1/ATR/Chk1 DNA damage response pathway. The data also support the inclusion of patients with PDAC in clinical studies of 9-ING-41 alone and in combination with gemcitabine.

Introduction

Pancreatic ductal adenocarcinoma (PDAC), which constitutes 93% of pancreatic cancers, is predicted to be the second leading cause of cancer-related deaths in the United States by 2030 (1, 2). The 5-year relative survival rate of all stages combined PDAC patients is less than 10% (3). As a standard therapy for locally advanced and metastatic pancreatic cancer, gemcitabine has a 5.4% partial response rate (4) and the great preponderance of initially sensitive tumors develop overt chemoresistance within weeks (5). FOLFIRINOX (folinic acid, fluorouracil, irinotecan, and oxaliplatin) and Nab-paclitaxel in combination with gemcitabine represent modest improvements over single-agent gemcitabine (6, 7). Novel approaches are thus urgently needed for patients with PDAC as are mechanism-based discovery of new therapeutic strategies to overcome chemotherapy resistance (8).

Glycogen synthase kinase-3 (GSK-3) α and β are highly conserved serine–threonine kinases initially described as key enzymes in regulating glycogen metabolism, with critical roles in Wnt/β-catenin signaling, immune regulation, and maintenance of stem cell identity (9, 10). We have previously shown that GSK-3β expression is regulated by oncogenic KRas signaling and its overexpression together with nuclear accumulation correlated with moderately and poorly differentiated pancreatic tumors (11–13). We found that GSK-3β promoted cell proliferation and survival through the regulation of NF-κB–dependent gene transcription (12). Consistent with this growth promoting effect of GSK-3β in PDAC, pharmacologic inhibition or genetic depletion of GSK-3β limited pancreatic cancer cell viability *in vitro* and suppressed tumor growth *in vivo* (11, 14, 15). Using a genetically engineered mouse model we demonstrated that GSK-3β contributes to KRas-driven tumor-promoting pathways that are required for the initiation of acinar-to-ductal

[1]The Division of Oncology Research, Schulze Center for Novel Therapeutics, Mayo Clinic, Rochester, Minnesota. [2]Department of Biochemistry and Molecular Biology, Mayo Clinic, Jacksonville, Florida. [3]Actuate Therapeutics Inc., Fort Worth, Texas. [4]Center for Precision Medicine, The First Affiliated Hospital of Wenzhou Medical University, Institute of Life Science, Wenzhou University, Zhejiang, China. [5]Starwise Therapeutics LLC, Madison, Wisconsin. [6]Monopar Therapeutics Inc., Wilmette, Illinois.

Note: Supplementary data for this article are available at Clinical Cancer Research Online (http://clincancerres.aacrjournals.org/).

Corresponding Author: Daniel D. Billadeau, Mayo Clinic, 200 First ST SW, Rochester, MN 55905. Phone: 507-266-4334; Fax: 507-266-5146; E-mail: Billadeau.Daniel@mayo.edu

Clin Cancer Res 2019;XX:XX–XX

doi: 10.1158/1078-0432.CCR-19-0799

Published OnlineFirst September 18, 2019; DOI: 10.1158/1078-0432.CCR-19-0799

Translational Relevance

Pancreatic ductal adenocarcinoma (PDAC) is a genetically heterogeneous, incurable, intensely chemoresistant malignancy. Glycogen synthase kinase 3β (GSK3β) is an emerging therapeutic target in a spectrum of human malignancies, including PDAC. The data presented herein demonstrate a previously uncharacterized role for GSK3β in the regulation of the TopBP1/ATR/Chk1 DNA damage response pathway. Treatment with the GSK-3 inhibitor 9-ING-41 sensitized PDAC cells to gemcitabine, as well as liposomal irinotecan *in vivo*. As 9-ING-41 has recently entered clinical studies, our data highlight not only a novel mechanism of action for 9-ING-41, but also provide a compelling rationale for the inclusion of patients with PDAC in clinical studies of 9-ING-41 in combination with gemcitabine/abraxane or MM398. These data also support the study of 9-ING-41 with other agents that induce an ATR-mediated DNA damage response.

metaplasia (16). These data support the potential therapeutic benefit of targeting GSK-3 in human pancreatic cancer.

GSK-3 inhibitor tool compounds have been developed and tested for their abilities to sensitize pancreatic cancer cells to gemcitabine. Previous studies in hematopoietic cells (17) and pancreatic cancer cells (18) showed that activation of the Akt–GSK–3β pathway is a key signaling event for gemcitabine resistance. The GSK-3β inhibitor tool compound Bio (19) could prevent the sensitization to gemcitabine-induced cell death by zidovudine (18). Lithium, a GSK-3 inhibitor, synergistically enhances the anticancer effect of gemcitabine by promoting the ubiquitin-dependent proteasome degradation of Gli1 (20, 21). The GSK-3 inhibitor AR-A014418 (22) also sensitizes pancreatic cancer cells to gemcitabine with altered expression of genes involved in DNA repair (23). Interestingly, although GSK-3β inhibition could disrupt NF-κB activity in pancreatic cancer cells, it did not significantly sensitize these cells to gemcitabine (24). The GSK-3 inhibitor LY2090314 (25) was clinically evaluated in patients for metastatic pancreatic cancer [NCT01632306] but its adverse PK properties ended its development. We have shown that a series of novel GSK-3 inhibitors, from which the clinical candidate, 9-ING-41 emerged, impaired PDAC and ovarian cancer cell proliferation and survival *in vitro* (26, 27), but its effects on PDAC *in vivo* and mechanism of action are not known.

Herein, we provide evidence that 9-ING-41, which is currently being evaluated in a phase I/II trial in patients with advanced cancer, reduces proliferation of PDAC cells *in vitro* and xenografts *in vivo*, and significantly sensitizes them to gemcitabine. 9-ING-41 impairs the ATR/Chk1 DNA damage response (DDR) signaling pathway induced by gemcitabine. Mechanistically, we show that pharmacologic inhibition or genetic depletion of GSK-3β led to the degradation of TopBP1, a key molecule that is required for optimal ATR phosphorylation of Chk1 leading to S-phase arrest and DNA repair. These data describe a previously unrecognized role for GSK-3β in regulating the ATR–Chk1 DDR pathway and provide a compelling rationale for the inclusion of patients with PDAC in clinical studies of 9-ING-41 in combination with gemcitabine/abraxane or MM398.

Materials and Methods

Cell culture, reagents, and treatments

All the chemicals were obtained from Sigma unless otherwise specified. BxPC3, HupT3, Panc01, CFPAC-1, L3.6 were obtained from ATCC. Panc01 and CFPAC were maintained in DMEM medium. BxPC3 and HupT3 were maintained in RPMI1640 medium. L3.6 cells were maintained in MEM medium and supplemented with 1% nonessential MEM amino acids. Pancreatic cancer patient-derived xenografts (PDX) cell lines including 6741, 5160, 6413, and 4041 were developed from PDAC tissue resections that had been established in nude mice as described previously (28) and were maintained in DMEM-F12 medium. GSK-3β-null mouse embryonic fibroblasts (MEF) and matching wildtype MEFs were a kind gift from Dr. Jim Woodgett (Ontario Cancer Institute, Toronto, ON, Canada) and maintained in DMEM medium. All culture media were supplemented with 10% FBS, 1% L-glutamine and 1% penicillin streptomycin. Cells were counted and plated 24 hours before treatment. Mycoplasma Detection Kit was used for detecting mycoplasma contamination. The latest testing was performed on April 30, 2019. All cells used in the described experiments were collected within 5 passages. The GSK-3 inhibitor Bio (Selleckchem), 9-ING-41 (Actuate Therapeutics Inc.), gemcitabine (Eli Lily), Irinotecan liposomal formulation (IRT-LP; obtained from the Mayo Pharmacy) and MG132 (Sigma-Aldrich) were also used in this study.

MTS and clonogenic assay

Cell proliferation was measured by 3-(4,5-dimethylthiazol-2-yl)-5-(3-carboxymethoxyphenyl)-2-(4-sulfophenyl)-2H-tetrazolium) (MTS) assay (Promega). Briefly, 5,000 cells/well were seeded in a 96-well culture plates and incubated in culture medium with or without indicated drug treatments for 48 hours. Medium was removed, and fresh medium was added to each well along with 1:20 dilution of MTS solution. After 2 hours of incubation, the plates were analyzed with a microplate reader at a wavelength of 490 nm (Molecular Devices). To assess for potential drug synergy, the combination index (CI) was calculated using CalcuSyn (Biosoft). For clonogenic assays, cells were collected and seeded in 6-well plates at 1,500 cells/mL. After a 4-hour incubation, which allowed cells to attach, culture medium with or without indicated vehicle or drug treatments were added. Forty-eight hours later, supernatant in the wells were aspirated and washed with PBS (NaCl 0.137 M, KCl 2.7 mmol/L, Na_2HPO_4 8.1 mmol/L, KH_2PO_4 1.5 mmol/L, pH 7.4) to remove residual drug. Fresh medium was then added to allow colony formation. Colonies were grown until visible and counted after staining with Coomassie brilliant blue R (42% methanol, 16.8% acetic acid, 1 mg/mL Brilliant blue R).

Subcutaneous and orthotopic pancreatic cancer animal model

The evaluation of 9-ING-41 in combination with gemcitabine therapy in PDX pancreatic tumor model was carried out in the Center for Developmental Therapeutics, Northwestern University, Evanston, IL, as described previously (29). The pancreatic PDX tumor model PCF 379419 was transplanted subcutaneously into the flanks (left and right side) of nude mice (Jackson Laboratory). Three weeks after tumor transplantation, mice were randomized into 4 groups ($n = 3$/group) and treated with: Vehicle (DMSO), Gemcitabine (10 mg/kg in week 1 and 5 mg/kg in week 2 and 3), 9-ING-41 (40 mg/kg), or both Gemcitabine and 9-ING-41 twice a

Published OnlineFirst September 18, 2019; DOI: 10.1158/1078-0432.CCR-19-0799

week for 3 weeks by intraperitoneal injection. For orthotopic pancreatic cancer animal models, 6- to 8-week-old NSG male mice were procured from Charles River Laboratories and housed in the institutional animal facilities. All animal experiments had approval from the Institutional Animal Care and Use Committee of the Mayo Clinic. To establish an orthotopic pancreatic tumor model, approximately 1 million 6,741 PDX cells suspended in 100 μL PBS containing 20% matrigel were slowly injected orthotopically into the head pancreas. In the orthotopic studies, 9-ING-41 was diluted in PEG400/Tween80/Ethanol (PTE) at a ratio of 75:8:17. Prior to injection, an equal volume of saline was used to further dilute the sample. Three weeks following tumor cell implantation, mice were randomly divided into 4 groups ($n = 5$) and treated with: Vehicle (vehicle consisted of PTE), Gemcitabine (10 mg/kg), 9-ING-41 (40 mg/kg), or both Gemcitabine (10 mg/kg) and 9-ING-41 (40 mg/kg) twice a week for 4 weeks by intraperitoneal injection. In the combination group, gemcitabine was given 1 hour following 9-ING-41 injection. Tumor size was measured with calipers and tumor volume was calculated using the formula $1/2(\text{length} \times \text{width}^2)$. At the end of the study, tumors were collected, fixed in 10% formalin and embedded in paraffin. A similar experimental design was used for the survival study in which the PDX cell lines 4535, 4636, 6741, and 4911 were injected orthotopically. In this experiment, the treatment protocol was 2 chemotherapeutic injections per week for 4 weeks. An addition to this experiment was the use of IRT-LP at 15 mg/kg as well as the combination of 9-ING-41 and IRT-LP. Mice were subsequently monitored and euthanized when IACUC endpoint criteria were reached. The date of death was recorded from the end of last treatment.

Western blot analysis

Cells were lysed with Western lysis buffer (1% TritonX-100, 10 mmol/L Tris Base, 50 mmol/L NaCl, 5 mmol/L EDTA, 50 mmol/L NaF, 30 mmol/L $Na_4P_2O_7$ pH 7.4) supplemented with aprotinin, leupeptin, sodium orthovanadate, phenylmethylsulfonyl fluoride (PMSF), and calyculin A (Cell Signaling Technologies). Lysates were subjected to SDS-PAGE and immunoblotting as previously described (16). Antibodies used for immunoblotting and immunofluorescence are described in detail in Supplementary Table S1.

siRNA, plasmid construction, and transfection

Stealth siRNAs were purchased from Invitrogen (HSS104518 and HSS104519 for GSK-3α; HSS104522 and HSS104523 for GSK-3β) and transfected with Lipofectamine RNAiMAX reagent (Thermo Fisher Scientific) according to the manufacturer's instruction. MEF cells were transfected with Lipofectamine 2000 (Invitrogen) according to the manufacturer's instruction. GSK-3β suppression reexpression vectors have been described previously (30).

Lentiviral packaging transduction and selection of stable cells

Lentivirus packaging, cell infection, and selection of pLKO-shRNA stable cells were performed as previously described following institutional biosafety regulations (30). Briefly, L3.6 and 6741 cells were infected with appropriate amounts of lentiviral particle-containing medium. Twenty-four hours later, virus-containing medium was replaced with fresh medium supplemented with 2 μg/mL of puromycin. Pooled resistant clones were used for experiments.

Cell-cycle analysis, induction of cell-cycle arrest, and EdU labeling

For cell-cycle analysis, the treated cells were harvested, washed with PBS, and fixed with precooled 70% ethanol in the dark at −20°C for 1 hour. The fixed cells were then washed with PBS and treated with RNase I at 37°C for 30 minutes. Finally, the cells were stained with PI solution (20 μg/mL propidium iodide (PI) in 10% sodium citrate with 0.1% TritonX-100) at room temperature for an additional 15 minutes and analyzed on a FACSCanto II flow cytometer (BD Bioscience). Data were processed using Modfit (Verity Software). To arrest cell cycle at M phase, asynchronous cells were treated with 2 mmol/L thymidine (Sigma) for 24 hours. Then, the cells were released from the thymidine block for 3 hours by washing once with PBS and adding fresh culture medium. Finally, 100 ng/mL Nocodazole (Sigma) was added to the medium for 12 hours, and M-phase–arrested cells were collected by shaking. For EdU (5-ethynyl-2′-deoxyuridine) labeling, cells were treated with EdU at a concentration of 10 μmol/L for 1 hour before harvesting. Staining was performed by Click-iT EdU Alexa Fluor 488 Flow Cytometry Kit (Invitrogen). Cells were trypsinized (Invitrogen) and resuspended in 0.5% BSA in PBS and fixed with 4% paraformaldehyde. Cells were permeabilized and stained using the cocktail mixture outlined and provided by manufacturer. Stained cells were resuspended and analyzed on the FACSCanto II flow cytometer (BD Bioscience), and data were processed using FlowJo (TreeStar). The mean fluorescence intensity (MFI) was defined as the geometric mean of the given fluorescent probe.

Cell apoptosis and necrosis analysis

Apoptosis and necrosis of pancreatic cancer cells were measured as previously described (30). Briefly, the treated pancreatic cancer cells were detached by trypsinization and stained with annexin V labeled with APC (BD Bioscience) and PI (20 μg/mL; Sigma) for 15 minutes. Cells (50,000 per condition) were then analyzed on the FACSCanto II flow cytometer (BD Bioscience) and the fraction of cells positive for annexin V and/or PI was calculated using FlowJo (TreeStar).

Immunofluorescence staining

The 6741 PDAC cells were plated on coverslips and left to attach overnight. Cells were subsequently treated as indicated and fixed for IF studies to measure pS317 Chk1, gamma-H2Ax, and EdU-488. The percentage of EdU-488 positive cells was enumerated and the nuclear MFI of pS317, gamma-H2Ax, and EdU-488 were measured using the ImageJ open source image-processing package. Additionally, FPPE sections from 6741 orthotopic experiments were subjected to immunofluorescence staining for pS317 Chk1 as described previously (16, 31). The MFI for nuclear pS317 Chk1 was measured using ImageJ. Confocal images were collected with an LSM-800 laser scanning confocal microscope with a ×63-oil Plan-Apochromat objective lens using ZEN Blue 2.6 software package (Carl Zeiss).

Statistical analysis

Data are expressed as mean ± SEM and analyzed by repeated measures analysis of variance, 1-way ANOVA and unpaired Student *t* test using GraphPad Prism software (GraphPad Software Inc.). A value of $P < 0.05$ denotes statistical significance.

Published OnlineFirst September 18, 2019; DOI: 10.1158/1078-0432.CCR-19-0799

Results

9-ING-41 reduces growth of PDAC cells and sensitizes them to gemcitabine *in vitro*

The novel small-molecule ATP-competitive GSK-3 inhibitor 9-ING-41 has been shown to inhibit various human cancer cells growth *in vitro* and significantly increase tumor-killing effect when combined with chemotherapies in resistant glioblastoma and breast cancer (27, 29, 32, 33). To examine its antitumor proliferation effect on pancreatic cancer cells, 5 previously described PDAC cell lines (30) and 3 recently developed pancreatic cancer PDX (28) cell lines were plated and treated with 9-ING-41 in increasing nanomolar concentrations (50 to 2,000 nmol/L). Growth suppression was observed in all tested cell lines using a colorimetric, MTS assay after 48 hours (Fig. 1A). We next tested the effect of 9-ING-41 in combination with gemcitabine. Although 9-ING-41 alone inhibited 6741 proliferation at both 48 and 72 hours, it also synergistically sensitized 6741 (Fig. 1B) and 5160 (Supplementary Fig. S1A) to gemcitabine as determined by calculating the combination index. To further investigate the cancer cell killing and chemo-sensitizing effect of 9-ING-41, we

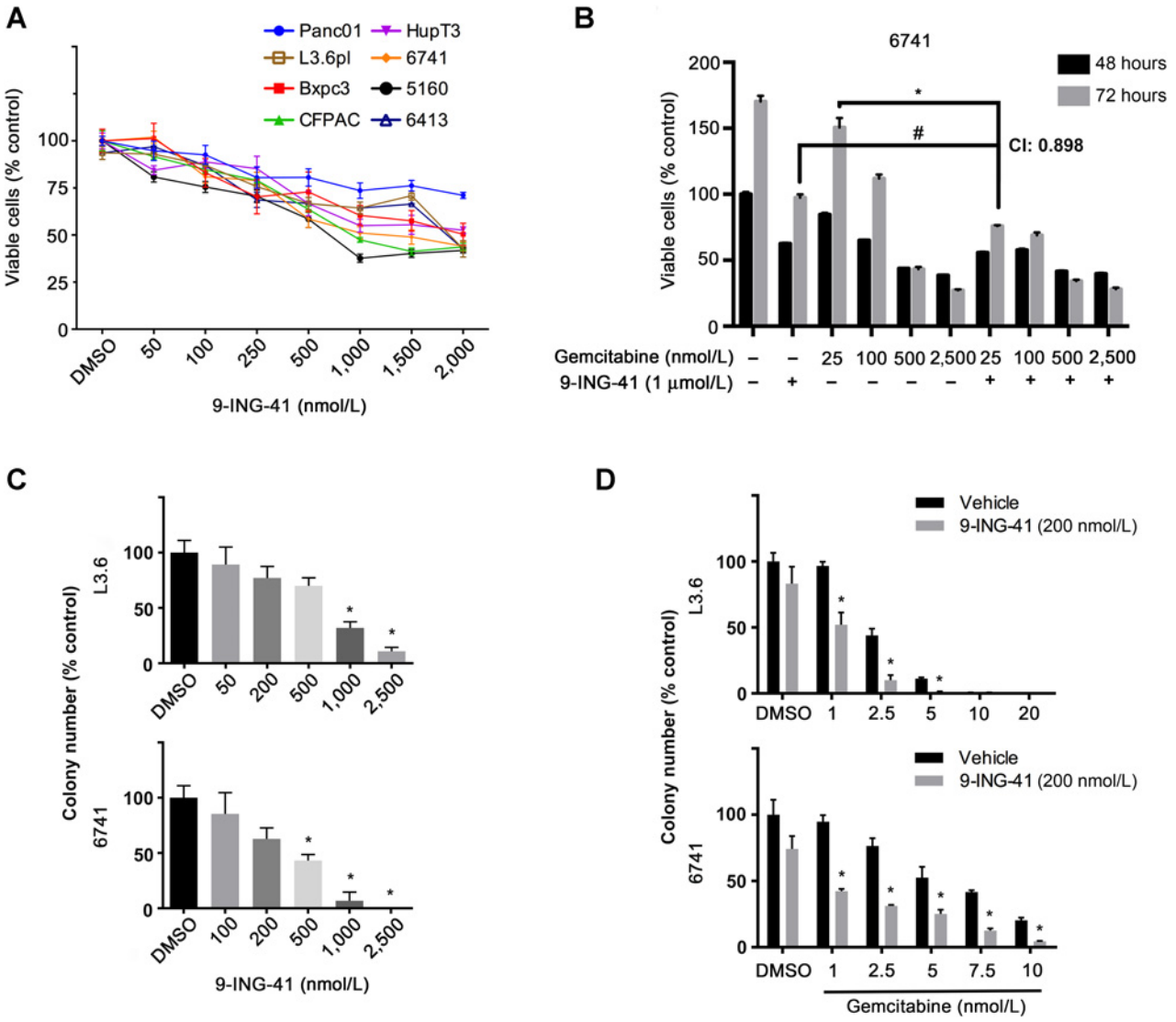

Figure 1.

9-ING-41 treatment synergizes with gemcitabine to abrogate PDAC cell proliferation and colony formation *in vitro*. **A,** The indicated PDAC cell lines were seeded in 96-well plates and treated with DMSO or increasing concentration of 9-ING-41 (nmol/L) for 48 hours. Cell proliferation was determined by MTS assay. Data were quantified as percentage of control and expressed as mean ± SEM; $n = 6$. **B,** The 6741 PDX-derived cell line was plated and treated with 1 μmol/L 9-ING-41 alone or with increasing concentrations of gemcitabine (nmol/L) for 48 and 72 hours. Cell proliferation was determined by MTS assay. Data were quantified as percentage of control and expressed as mean ± SE. *, $P < 0.05$ gemcitabine and 9-ING-41 combinations versus gemcitabine alone. #, $P < 0.05$ gemcitabine and 9-ING-41 combination versus 9-ING-41; $n = 6$. **C,** L3.6 and 6741 PDAC cells were seeded in 6-well plate and treated with DMSO or increasing concentration of 9-ING-41 (nmol/L) for 48 hours. Supernatant was then removed and remaining cells were allowed to form colonies. Colony number from triplicate samples were counted and expressed as mean ± SEM. *, $P < 0.05$ 9-ING-41 versus DMSO. **D,** Clonogenic assay was carried out as described in **C** but 200 nmol/L 9-ING-41 was added together with increasing concentration of gemcitabine. Colony number from triplicate samples were counted and expressed as mean ± SEM. *, $P < 0.05$ gemcitabine and 9-ING-41 combination versus gemcitabine alone.

Published OnlineFirst September 18, 2019; DOI: 10.1158/1078-0432.CCR-19-0799

utilized L3.6 and 6741 in a clonogenic assay (Supplementary Fig. S1B and S1C). L3.6 and 6741 colony numbers decreased in a dose-dependent manner following 9-ING-41 treatment (Fig. 1C). When combined with increasing doses of gemcitabine, 9-ING-41 could substantially reduce colony number compared with gemcitabine alone (Fig. 1D). Previous studies have shown that 9-ING-41 treatment inhibited the proliferation of ovarian cancer cell lines by induction of apoptosis (27). Therefore, we examined cell apoptosis/necrosis by annexin V/PI staining in 9-ING-41-treated pancreatic cancer cells. As shown in Supplementary Fig. S2A and S2B, combination of both 9-ING-41 and gemcitabine decreased the number of live cells and increased the population of necrotic cells. Immunoblotting results further confirmed the phenotype of significant cell death in the combination drug group (Supplementary Fig. S2C). Taken together, these data suggest that 9-ING-41 can suppress cell proliferation and sensitize PDAC cells to gemcitabine *in vitro*.

The combination of 9-ING-41 and gemcitabine limits tumor growth *in vivo*

To better understand the antitumor effect of 9-ING-41 alone and in combination with gemcitabine *in vivo*, we first tested 9-ING-41 using the PDAC PDX model PCF379419. As shown in Fig. 2A, the PDX tumor expanded aggressively in the vehicle and 9-ING-41-treated animals, whereas monotherapy with gemcitabine suppressed, but did not completely block tumor growth. In contrast, the combination treatment with 9-ING-41 and gemcitabine caused a profound decrease in tumor growth, ending with notable regression after 3 weeks of treatment (Fig. 2A and B).

We next evaluated the effect of 9-ING-41 using an orthotopic tumor mouse model (34). The 6741 PDAC cell line was implanted into the head of the pancreas and allowed to grow until tumors were palpable. Mice were then randomized into treatment groups and treated twice a week for 4 weeks (Fig. 2C). Two days following the last round of therapy, orthotopic tumors were isolated and tumor weight and volume were measured. Although we did observe a statistically significant inhibition of tumor growth with monotherapy treatment in the orthotopic model when compared with vehicle, consistent with the subcutaneous model, we observed a greater reduction in tumor weight and tumor volume in animals that received combination therapy when compared with either vehicle or monotherapy (Fig. 2D). Finally, we orthotopically implanted 6741 and 3 additional PDX-derived tumor cell lines (4535, 4636, and 4911) and assessed survival following individual or combination drug treatments. In addition to using gemcitabine, we also used

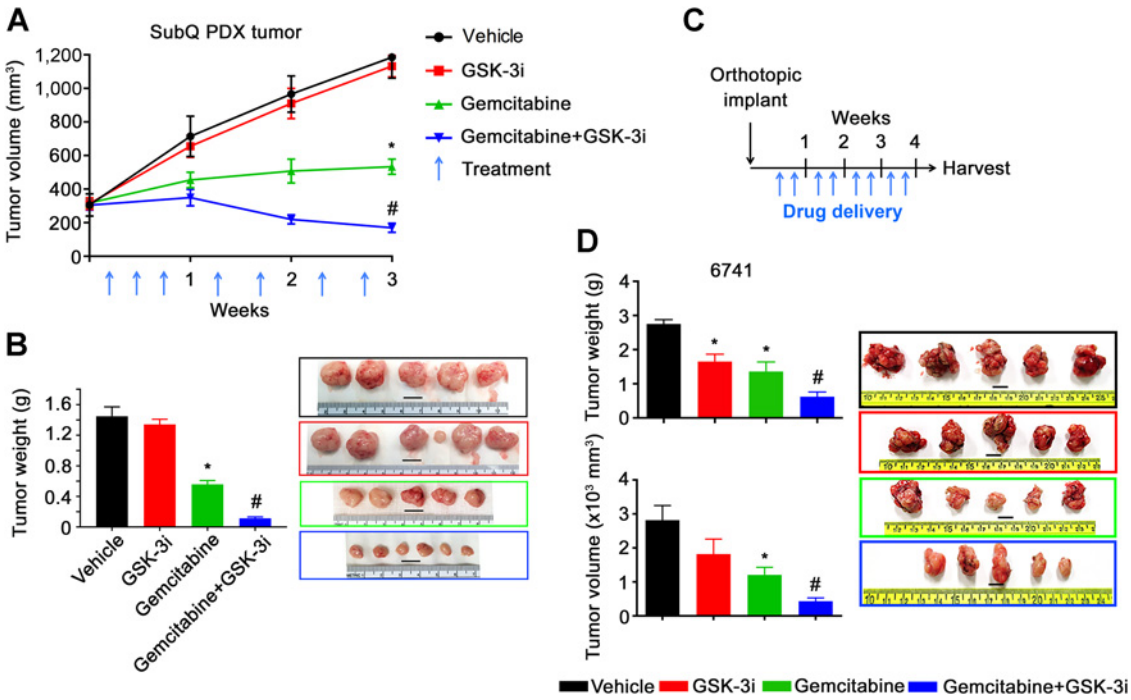

Figure 2.

9-ING-41 (GSK-3i) and Gemcitabine abrogate tumor growth *in vivo*. **A,** The pancreatic PDX tumor (PCF 379419) was transplanted subcutaneously into both flanks of athymic nude mice (12 mice in total). Tumors were size matched and mice were randomized into 4 treatment groups: Vehicle, Gemcitabine, 9-ING-41 (40 mg/kg) and Gemcitabine + 9-ING-41. Gemcitabine was used as 10 mg/kg (week 1) and 5 mg/kg (week 2 and 3). Vehicle or drugs were injected intraperitoneally. Tumor volume was measured weekly and shown as mean ± SEM. ($n = 3$/group). *, $P < 0.05$ gemcitabine versus vehicle; #, $P < 0.01$ 9-ING-41 + gemcitabine versus gemcitabine alone. **B,** Tumors were removed and weighed at the end of the study and representative images of the PDX tumors from each group of animals are shown. *, $P < 0.05$ gemcitabine versus vehicle; #,$P < 0.05$ 9-ING-41 + gemcitabine versus gemcitabine alone. The weight of resected tumors were shown as mean ± SEM. One tumor from each of the vehicle, 9-ING-41 and gemcitabine treatment groups did not grow and was thus excluded from the analysis. Bar, 1 cm. **C,** Three weeks following orthotopic implantation of 6741 cells into the head of the pancreas, mice were randomly divided into 4 groups ($n = 5$/group) and treated with the indicated drugs [Vehicle, Gemcitabine (10 mg/kg), 9-ING-41 (40 mg/kg) and Gemcitabine + 9-ING-41] by intraperitoneal injection twice per week for 4 weeks as shown. **D,** At the end of week 4, tumors were removed and tumor weight and tumor volume were measured. *, $P < 0.05$ gemcitabine or 9-ING-41 monotherapy versus vehicle; #, $P < 0.05$ 9-ING-41 + gemcitabine versus gemcitabine alone. Images of the resected tumors are shown. Data were expressed as mean ± SEM; $n = 5$. Bar, 1 cm.

Published OnlineFirst September 18, 2019; DOI: 10.1158/1078-0432.CCR-19-0799

liposomal-formulated irinotecan (IRT-LP) to assess whether 9-ING-41 would also show increased efficacy when combined with this recently approved therapy for PDAC. Following implantation of the tumors, mice were monitored for tumor growth and then randomized and treated twice a week for 4 weeks (Supplementary Fig. S3A). Following the 4-week treatment, animals were monitored and euthanized when IACUC endpoints were met. All 4 vehicle-treated animals succumb to their tumors within 1-week following treatment, whereas animals treated with 9-ING-41, gemcitabine, or IRT-LP monotherapy survived slightly longer and varied by cell line and their sensitivity to gemcitabine or IRT-LP (Supplementary Fig. S3B). Combining 9-ING-41 with either gemcitabine or IRT-LP significantly extended survival compared with the monotherapy treatment in all 4-cell line models examined (Supplementary Fig. S3B). Taken together, these *in vivo* studies suggest that patients with PDAC may benefit from the combination of 9-ING-41 with existing chemotherapies.

GSK3 inhibition impairs gemcitabine induced Chk1 activation in PDAC cells

We next sought to understand the mechanism by which 9-ING-41 could sensitize PDAC cells to gemcitabine. Because gemcitabine induces the DDR pathway through activation of ATR, we initially investigated the phosphorylation of Chk1 (an ATR target) at S345 following gemcitabine treatment. As expected, gemcitabine treatment induced a time-dependent increase in Chk1 S345 phosphorylation in all cell lines examined (Fig. 3A). Consistent with our previous study (26, 27), 9-ING-41 increased the inhibitory phosphorylation of GSK-3β at serine 9 in pancreatic cancer cells (Supplementary Fig. S4A). We next investigated whether treatment with 9-ING-41 or a tool compound GSK-3 inhibitor, Bio, could impair gemcitabine-induced phosphorylation of Chk1. Significantly, a 2-hour pretreatment with either 9-ING-41 or Bio abrogated the gemcitabine-induced phosphorylation of Chk1 at both S317 and

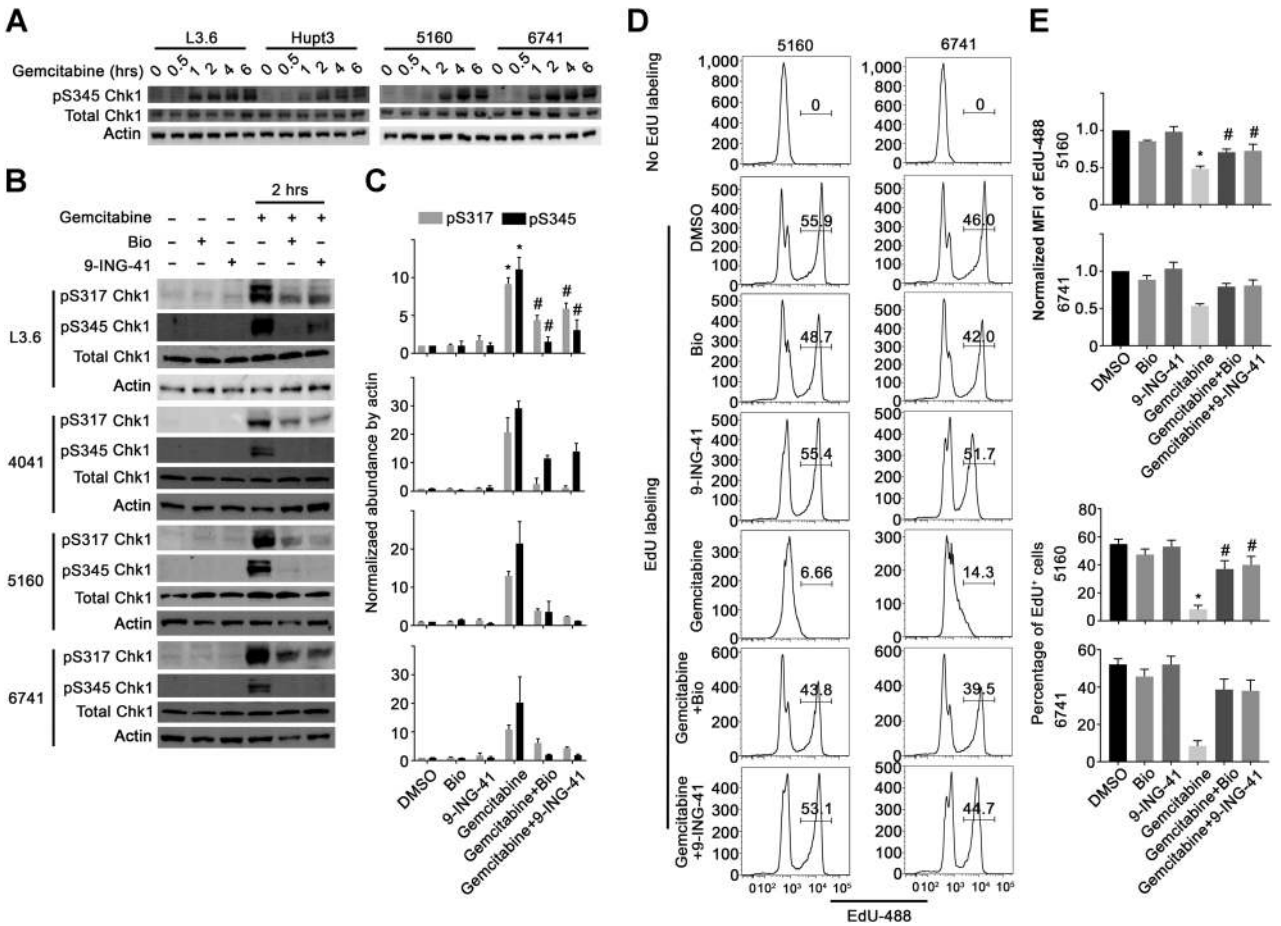

Figure 3.

GSK-3 abrogates gemcitabine-induced Chk1 activation and cell-cycle arrest. **A,** PDAC cell lines were treated with gemcitabine (500 nmol/L) over the indicated time course, harvested, and lysates were prepared and immunoblotted with the indicated antibodies. **B,** PDAC cell lines were pretreated with GSK-3 inhibitors Bio (5 μmol/L) or 9-ING-41 (5 μmol/L) for 2 hours followed by an additional 2-hour treatment with gemcitabine (500 nmol/L). Phosphorylated Chk1 at S317 and S345 Chk1, as well as total Chk1 were examined by immunoblotting. β-Actin was used as a loading control. **C,** Average signal intensity of pS317 and pS345 Chk1 were analyzed and expressed as mean ± SEM. *, $P < 0.05$ gemcitabine versus DMSO. #, $P < 0.05$ gemcitabine and 9-ING-41 versus gemcitabine alone. Data are representative of 3 independent experiments. **D,** 5160 and 6741 were treated as indicated in **B** and then provided EdU for 1 hour prior to harvesting. EdU incorporation was detected using the EdU Detection Kit followed by flow cytometry. **E,** EdU-positive cells were gated and the MFI of the EdU peak is graphically displayed. **E,** The normalized MFI and percentage of EdU-488-positive cells were quantified and expressed as mean ± SEM. *, $P < 0.05$ gemcitabine versus DMSO. #, $P < 0.05$ gemcitabine and GSK-3 inhibitor versus gemcitabine alone. Data presented in **D** and **E** is representative of 3 independent experiments.

Published OnlineFirst September 18, 2019; DOI: 10.1158/1078-0432.CCR-19-0799

S345 (Fig. 3B and C). Although it has been shown that Chk1 is a negative regulator of polo-like kinase 1 (PLK1; ref. 35), we only detected a slight change in PLK1 phosphorylation (Supplementary Fig. S4B). Consistent with activation of Chk1 induced by gemcitabine, cell-cycle analysis by PI staining showed significantly increased G_1–S and decreased G_2–M population in gemcitabine-treated group, whereas GSK-3 inhibition partially abolished the cell-cycle arrest (Supplementary Fig. S5A). To further evaluate whether GSK-3 inhibition restored cell-cycle progression, we monitored EdU incorporation into cells actively synthesizing DNA. Although neither vehicle nor GSK-3 inhibitor treatment affected EdU incorporation, as expected, treatment with gemcitabine led to decreased EdU incorporation in all 3 PDAC cell lines tested (Fig. 3D and E; Supplementary Fig. S5C and S5D). In contrast, pretreatment with either GSK-3 inhibitor prevented the gemcitabine-induced S-phase arrest (Fig. 3D and E; Supplementary Fig. S5C and S5D). Taken together, these data indicate that GSK-3 inhibition abrogates the activation of the ATR-Chk1 DDR leading to S-phase arrest.

GSK-3β regulates the ATR–Chk1 signaling pathway

Because 9-ING-41 and Bio are not totally selective for GSK-3β or GSK-3α, we next sought to determine which of these 2 kinases participated in the activation of the ATR–Chk1 pathway. To accomplish this, we depleted GSK-3β or GSK-3α in PDAC cell lines using siRNA and examined the phosphorylation of Chk1 following gemcitabine treatment. As can be seen in Fig. 4A, depletion of either GSK-3 kinase led to a reduction in gemcitabine-induced Chk1 phosphorylation, with GSK-3β depletion having a more pronounced effect. Because the effect on Chk1 phosphorylation was impacted more by GSK-3β depletion, we next constructed stable GSK-3β knockdown L3.6 and 6741 cells (Fig. 4B). Similar to the siRNA knockdown results, depletion of GSK3β showed a significant effect on Chk1 phosphorylation following gemcitabine treatment when compared with shVector control cells (Fig. 4B). Consistent with these results, GSK-3β knockout mouse embryonic fibroblasts (MEF) transfected with an empty Flag-Vector exhibited remarkable reduction of phosphorylated Chk1 after gemcitabine treatment compared with wild-type (WT) MEF cells (Fig. 4C). Significantly, re-expression

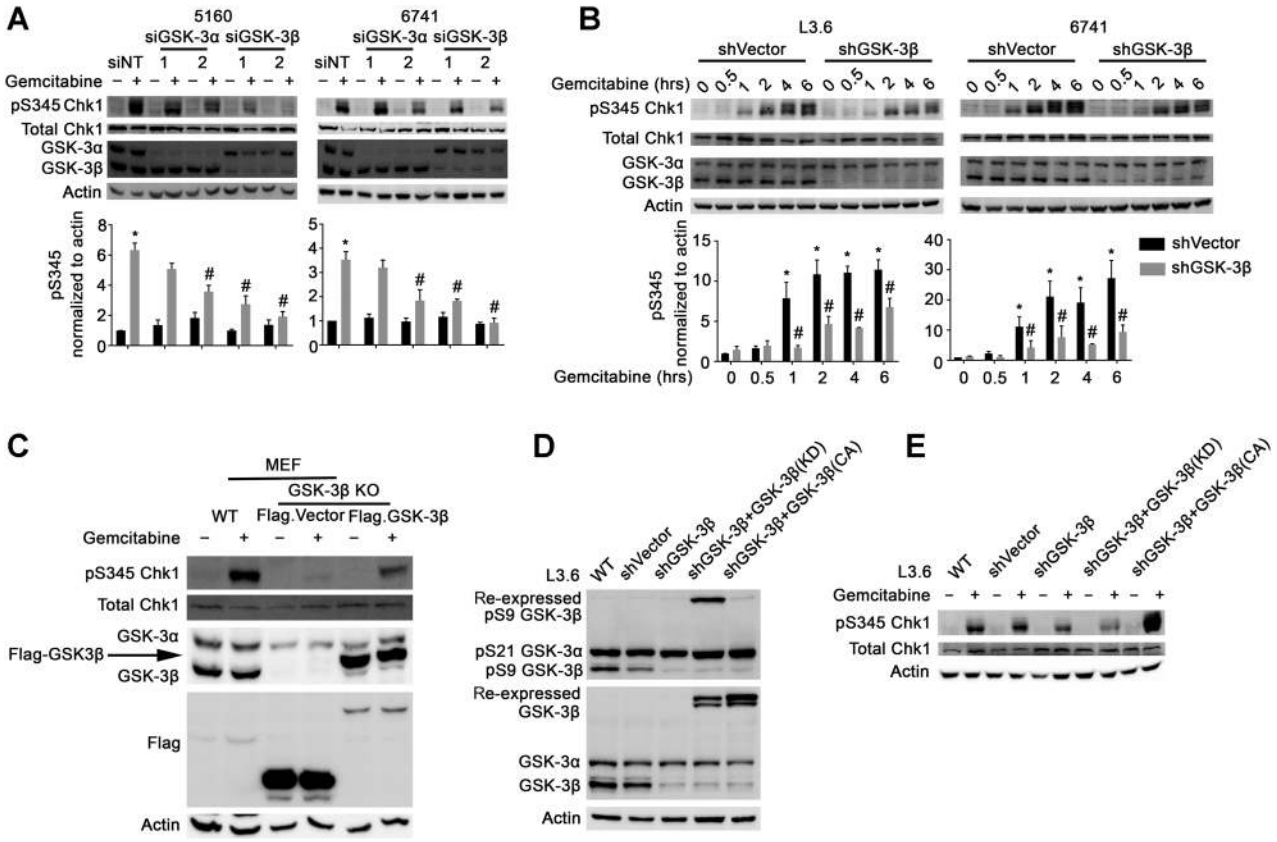

Figure 4.

GSK-3β regulates ATR-dependent phosphorylation of Chk1 in response to gemcitabine treatment. **A,** PDAC cell lines were depleted of GSK-3α or GSK-3β using siRNA and then treated with gemcitabine (500 nmol/L) for 2 hours. Cell lysates were prepared and immunoblotted with the indicated antibodies. Average signal intensity of pS345 Chk1 was analyzed and expressed as mean ± SEM. *, $P < 0.05$ gemcitabine versus DMSO. #, $P < 0.05$ siGSK-3 versus siNT after gemcitabine; $n = 3$. **B,** L3.6 and 6741 PDAC cell lines stably depleted of GSK-3β were treated with gemcitabine (500 nmol/L) for 2 hours. Protein lysates were prepared and immunoblotted as indicated. Average signal intensity of pS345 Chk1 was analyzed and expressed as mean ± SEM. *, $P < 0.05$ gemcitabine versus DMSO in shVector cells. #, $P < 0.05$ shGSK-3β versus shVector cells after gemcitabine; $n = 3$. **C,** WT or GSK-3β KO MEFs were left untransfected or transfected with vector control or WT GSK-3β and treated with gemcitabine (500 nmol/L) for 2 hours. Protein lysates were prepared and immunoblotted as indicated. **D** and **E,** L3.6 cells were left uninfected or were infected with a control lentivirus or one that stably depletes GSK-3β and re-expresses a nontargetable kinase-dead or constitutively active GSK-3β cDNA. Cells were then treated with gemcitabine (500 nmol/L) for 2 hours, protein lysates were obtained and immunoblotted as indicated.

Published OnlineFirst September 18, 2019; DOI: 10.1158/1078-0432.CCR-19-0799

of Flag-GSK-3β in GSK-3β knockout cells rescued Chk1 phosphorylation (Fig. 4C). Finally, L3.6 cells engineered to be stably depleted of GSK-3β and expressing either kinase-dead or constitutively active GSK-3β were assessed for gemcitabine-induced activation of Chk1. As can be seen in Fig. 4D and E, stable knockdown of GSK-3β impacted gemcitabine-induced phosphorylation of Chk1, which was not rescued by re-expression of kinase-dead GSK-3β, but was substantially restored in cells expressing constitutively active GSK-3β. Altogether, these data provide genetic evidence that GSK-3β, and to some extent GSK-3α, regulate the gemcitabine-induced DDR signaling pathway leading to ATR–Chk1 activation.

GSK-3 contributes to Chk1 activation through stabilization of TopBP1

ATR-dependent phosphorylation of Chk1 during DNA replication stress depends upon several other signaling proteins including ATR interacting protein (ATRIP), and the trimetric Rad9-Hus1-Rad1 (9-1-1) clamp and topoisomerase IIβ binding protein (TopBP1; ref. 36). To determine the mechanism by which GSK-3 inhibition impacts ATR-Chk1 activation, we examined the protein levels of TopBP1, ATR, and ATRIP following GSK-3 inhibitor treatment. As can be seen in Fig. 5A, treatment of PDAC cell lines with either GSK-3 inhibitor did not affect the levels of ATR or ATRIP, but did lead to substantially reduced levels of TopBP1. Moreover, siRNA knockdown of GSK-3β led to a reduction in TopBP1 protein levels (Fig. 5B). It has been shown that Claspin is also required for ATR–Chk1 activation downstream of TopBP1 (37). However, we did not observe any change in Claspin protein levels following GSK-3 inhibitor treatment (Supplementary Fig. S6A).

It was recently shown that TopBP1 plays a crucial role in the maintenance of genomic integrity through the induction of DNA damage repair pathways (38, 39). Therefore, we performed immunofluorescent staining of gamma-H2Ax on cells 48 hours following the withdrawal of a 2-hour gemcitabine treatment in the presence or absence of 9-ING-41. Significantly, GSK-3 inhibition increased DNA damage and impaired DNA damage repair in pancreatic cancer cells (Supplementary Fig. S6B and S6C). Because it was shown that TopBP1 is degraded in a proteasome-dependent manner (40), we treated 5160 cells with 9-ING-41 in the presence or absence of the proteasome inhibitor MG132. Although 9-ING-41 treatment resulted in a decrease in TopBP1 protein levels, the cotreatment of 9-ING-41 and MG132 rescued TopBP1 protein levels (Fig. 5C). Finally, using the L3.6 reconstituted cell line we found that constitutively active but not kinase-dead GSK-3β could rescue TopBP1 protein levels (Fig. 5D). Taken together, these data suggest that GSK-3 kinase activity is required to stabilize the TopBP1 protein.

9-ING-41 decreases pS317 Chk1 levels in gemcitabine-treated animals

We next assessed whether 9-ING-41 could reduce phospho-Chk1 levels in tissues from gemcitabine-treated animals. Initially, we performed EdU incorporation and stained 6741 cells with anti-pChk1 (pS317) that had been treated with control,

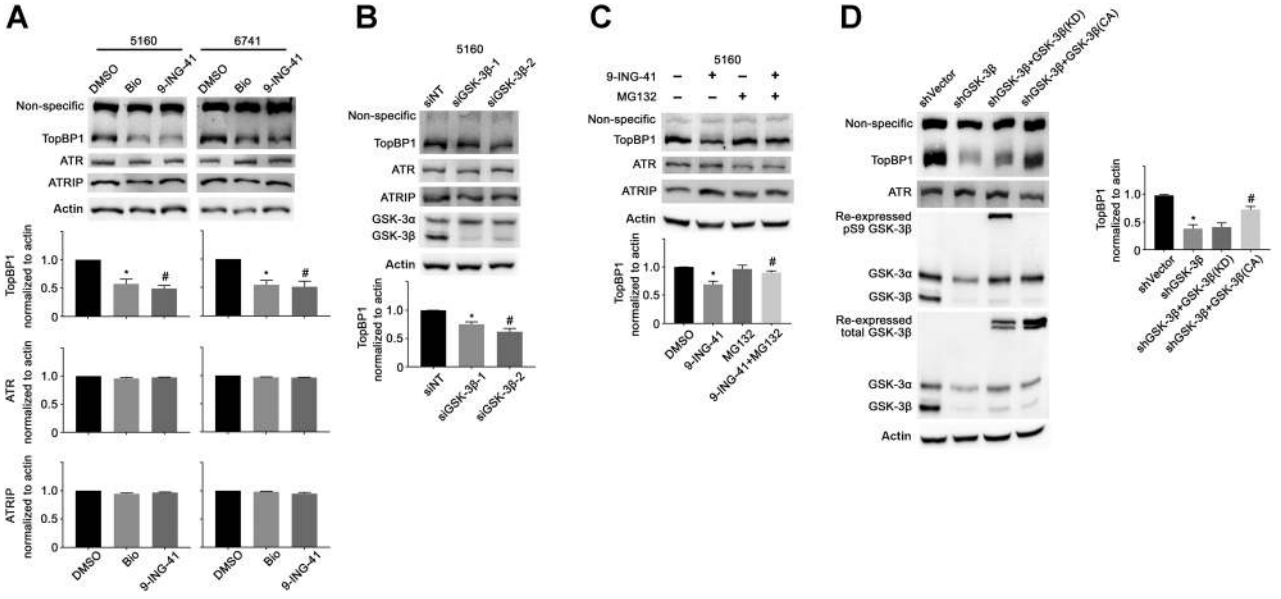

Figure 5.

GSK-3β regulates TopBP1 protein stability. **A,** 5160 and 6741 cell lines were treated with the GSK-3 inhibitors Bio (5 μmol/L) and 9-ING-41 (5 μmol/L) for 4 hours. Protein lysates were prepared and immunoblotted with the indicated antibodies. The average signal intensity of TopBP1, ATR and ATRIP were analyzed and expressed as mean ± SEM. *, $P < 0.05$ Bio versus DMSO. #, $P < 0.05$ 9-ING-41 versus DMSO; $n = 3$. **B,** Protein lysates were prepared from 5160 cells transfected with control siRNA or siRNA targeting GSK-3β and immunoblotted with the indicated antibodies. The average signal intensity of TopBP1 was analyzed and expressed as mean ± SEM. *, $P < 0.05$ siGSK-3β-1 versus siNT. #, $P < 0.05$ siGSK-3β-2 versus siNT; $n = 3$. **C,** The 5160 cell line was treated with 9-ING-41 (5 μmol/L) with or without MG132 (10 μmol/L) for 4 hours. Cell lysates were prepared and immunoblotted with the indicated antibodies. The average signal intensity of TopBP1 was analyzed and expressed as mean ± SEM. *, $P < 0.05$ 9-ING-41 versus DMSO. #, $P < 0.05$ 9-ING-41 and MG132 combination versus 9-ING-41; $n = 3$. **D,** Cell lysates were prepared from the panel of L3.6 cell lines described in Fig. 4D and immunoblotted with the indicated antibodies. The average signal intensity of TopBP1 was analyzed and expressed as mean ± SEM. *, $P < 0.05$ shGSK-3β versus shVector cells. #, $P < 0.05$ shGSK-3β with GSK-3β (**CA**) versus shGSK-3β cells. $n = 3$.

Published OnlineFirst September 18, 2019; DOI: 10.1158/1078-0432.CCR-19-0799

gemcitabine, 9-ING-41, or combination therapy. Consistent with our immunoblotting and flow cytometry data, phosphorylation of Chk1 at S317 was induced in response to gemcitabine together with dramatic loss of EdU positive cells as compared with DMSO or 9-ING-41-treated cells (Fig. 6A and B). Significantly, 6741 cells treated with the combination of 9-ING-41 and gemcitabine showed diminished Chk1 phosphorylation and restored EdU incorporation (Fig. 6A and B). We next examined the utility of the pS317 Chk1 antibody in our tissues harvested from the orthotopic model. Although the tissue staining showed an overall increase in background pS317 staining, gemcitabine treatment led to increased pS317 nuclear staining when compared with vehicle- and 9-ING-41-treated mice (Fig. 6C and D). In contrast, animals treated with combination therapy showed lower levels of nuclear pS317 staining. Collectively, these results support the overall mechanism that 9-ING-41 treatment-impairs ATR-mediated activation of the DNA damage response leading to Chk1 phosphorylation.

Discussion

In this study, we have found that the combination of gemcitabine with the clinically relevant small molecule GSK-3 inhibitor, 9-ING-41, impacts PDAC tumor growth *in vitro* and *in vivo* and significantly prolongs survival of mice bearing orthotopic tumors. Mechanistically, we identify a previously unknown role for GSK-3β kinase activity, and to a lesser extent GSK-3α, in the regulation of the ATR–Chk1 DDR signaling pathway through the stabilization of the critical adaptor molecule TopBP1 (Fig. 7). These findings suggest that 9-ING-41 should be studied in combination with gemcitabine or liposomal-formulated irinotecan for first-line therapy in patients with PDAC. Moreover, our data indicate that 9-ING-41 may overcome gemcitabine resistance in pancreatic cancer.

Although GSK-3β has sometimes been proposed to act as a tumor suppressor in various cancer types through its ability to phosphorylate pro-oncogenic molecules, for example c-Jun, c-Myc, cyclin D1, and β-catenin, leading to their proteasomal degradation (41), we and others have previously demonstrated that GSK-3β is overexpressed in many human malignancies including PDAC, and can be targeted for therapeutic intervention (11, 27, 29, 32, 33, 42). Indeed, in pancreatic cancer, GSK-3 has been implicated in the initiation of pancreatic cancer precursor lesions (16), resistance to chemotherapy (23) and overexpression correlated with reduced survival (21, 30, 12). Herein, we show that the combination of 9-ING-41 with gemcitabine can significantly enhance the survival and tumor killing effect *in vivo*. Recently, we have also shown that 9-ING-41 can overcome chemoresistance in breast cancer (33), impair tumor growth in renal cell cancer (32), neuroblastoma (43), and glioblastoma (29) suggesting that this clinically-relevant compound could be paired with other chemotherapies to treat several different human malignancies.

The DNA damage response pathway is a signaling network that senses different types of damage and coordinates a response that includes activation of transcription, cell-cycle control, apoptosis, senescence, and DNA repair (44). ATR along with its regulator ATRIP sense single-stranded DNA (ssDNA) such as the ssDNA present at stalled replication forks induced by gemcitabine (45). Chk1 is one of the established substrates for ATR that initiates a

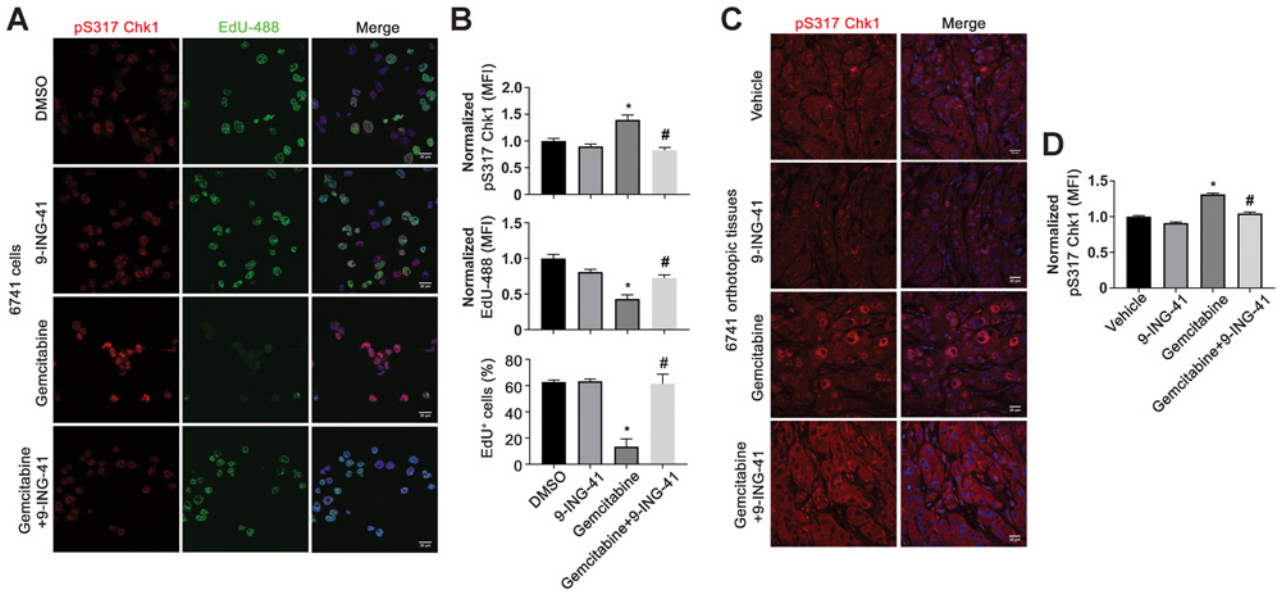

Figure 6.

9-ING-41 reverses Chk1 phosphorylation induced by gemcitabine treatment. **A,** 6741 cells were grown on coverslips, treated with DMSO, 9-ING-41 (5 μmol/L), gemcitabine (500 nmol/L), or the combination of 9-ING-41 and gemcitabine and pulsed with EdU 1 hour prior to fixation. Fixed cells were subsequently stained with anti-pS317 Chk1 antibodies and detected with an Alexa Fluor 568 conjugated donkey-anti-rabbit secondary (red) and EdU-488 (green). DNA was visualized following Hoechst staining (blue). **B,** The normalized MFI of nuclear pS317 Chk1, EdU-488, and the percentage of EdU-positive cells were evaluated by ImageJ and expressed as mean ± SEM. *, $P < 0.05$ gemcitabine versus DMSO. #, $P < 0.05$ gemcitabine and 9-ING-41 versus gemcitabine alone. $n = 200$ cells per treatment group. **C,** Immunofluorescence staining of pS317 Chk1 (red) and Hoechst (blue) from orthotopic 6741 PDX tumor tissue sections treated as described in Fig. 2D. **D,** The normalized MFI of pS317 Chk1 within the nucleus was evaluated by ImageJ and expressed as mean ± SEM. *, $P < 0.05$ gemcitabine versus Vehicle. #, $P < 0.05$ gemcitabine and 9-ING-41 versus gemcitabine. $n = 200$ cells per treatment group.

Published OnlineFirst September 18, 2019; DOI: 10.1158/1078-0432.CCR-19-0799

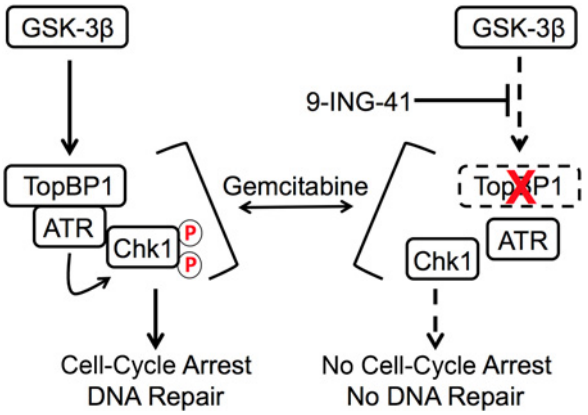

Figure 7.

Proposed model by which GSK-3 inhibition by 9-ING-41 disrupts the TopBP1/ATR/Chk1 pathway. In response to gemcitabine-induced DNA replication stress, TopBP1/ATR/ATRIP (not shown) complexes are recruited to stalled replication forks where ATR can fully activate Chk1 leading to cell cycle arrest and DNA repair. In the presence of 9-ING-41, TopBP1 protein levels are destabilized thus abrogating the full activation of ATR leading to reduced Chk1 phosphorylation and ultimately impaired cell-cycle arrest and likely DNA repair. Circle with red *P* indicates phosphorylation. Dashed rectangle with red X indicates TopBP1 degradation.

secondary wave of phosphorylation events that impact signaling networks leading to cell-cycle arrest and DNA repair (46). Several studies have shown that cancer cells lacking ATR or Chk1 are vulnerable to chemotherapeutics including gemcitabine and cytarabine highlighting the possibility that inhibiting the ATR–Chk1 signaling pathway may sensitize tumor cells or overcome resistance to chemotherapies that induce this DNA damage checkpoint (47, 45). Recently, several studies using ATR or Chk1 inhibitors in combination with gemcitabine provided direct evidence that targeting ATR-Chk1 signaling could sensitize PDAC cells to gemcitabine (48, 49). Herein, we observed synergistic tumor killing when 9-ING-41 was combined with gemcitabine or IRT-LP. Surprisingly, we found that GSK-3 inhibition or genetic depletion of GSK-3β blocked the phosphorylation of Chk1 following gemcitabine addition. We further demonstrated that GSK-3β was involved in stabilizing TopBP1, a critical adaptor molecule that is recruited to stalled replication forks and involved in the full activation of ATR (50, 45). Although it is presently unclear how GSK-3β stabilizes TopBP1, our data suggest that it requires a phosphorylation event either directly on TopBP1 itself, or on another protein involved in TopBP1 stability. Regardless of the mechanism, our data provide new insight into the regulation of the TopBP1/ATR/Chk1 signaling cascade and add TopBP1 to the ever-growing list of proteins whose function/stability are regulated by GSK-3β.

In summary, our study identified a heretofore-unknown role for GSK-3β in the regulation of ATR-mediated DDR checkpoint signaling through the stabilization of TopBP1. Moreover, this study provides valuable preclinical data for the inclusion of patients with PDAC in studies of 9-ING-41 given in combination with chemotherapy.

Disclosure of Potential Conflicts of Interest

D.D. Billadeau and A. Ugolkov have ownership interests (including patents) in and are consultants/advisory board members for Actuate Therapeutics, Inc. D.M. Schmitt is an employee of and has ownership interests (including patents) at Actuate Therapeutics, Inc. F.J. Giles has ownership interests (including patents) at Actuate Therapeutics, Inc. A. Kozikowski has ownership interests (including patents) in Actuate Therapeutics, Inc. and StarWise Therapeutics. A.P. Mazar is a consultant/advisory board member for Actuate Therapeutics. No potential conflicts of interest were disclosed by the other authors.

Authors' Contributions

Conception and design: L. Ding, S. Kiers, J.-S. Zhang, F.J. Giles, D. Mukhopadhyay, D.D. Billadeau

Development of methodology: L. Ding, S. Kiers, O. Alekhina, J.-S. Zhang, D. Mukhopadhyay

Acquisition of data (provided animals, acquired and managed patients, provided facilities, etc.): L. Ding, V.S. Madamsetty, S. Kiers, O. Alekhina, A. Ugolkov, J. Dube, Y. Zhang, D. Mukhopadhyay, E. Wang, S.K. Dutta

Analysis and interpretation of data (e.g., statistical analysis, biostatistics, computational analysis): L. Ding, V.S. Madamsetty, S. Kiers, A. Ugolkov, F.J. Giles, A.P. Mazar, D. Mukhopadhyay, D.D. Billadeau

Writing, review, and/or revision of the manuscript: L. Ding, V.S. Madamsetty, A. Ugolkov, D.M. Schmitt, F.J. Giles, A.P. Mazar, D. Mukhopadhyay, D.D. Billadeau

Administrative, technical, or material support (i.e., reporting or organizing data, constructing databases): L. Ding

Study supervision: L. Ding, D.D. Billadeau

Other (invented drug used in the paper): A.P. Kozikowski

Other (his lab did all the early development work and advanced 9-ING-41 into the clinic. They provided input on all studies with regard to drug formulation, use, delivery and doses): A.P. Mazar

Acknowledgments

We would like to thank members of the Division of Oncology Research especially Drs. Scott Kaufmann, Larry Karnitz, Zhenkun Lou, as well as members of the Billadeau laboratory for helpful discussions. This work was supported by the Pancreatic Cancer SPORE grant CA102701 to D.D. Billadeau, and NIH grant CA150190 to D.M. Schmitt.

The costs of publication of this article were defrayed in part by the payment of page charges. This article must therefore be hereby marked *advertisement* in accordance with 18 U.S.C. Section 1734 solely to indicate this fact.

Received March 8, 2019; revised June 3, 2019; accepted August 2, 2019; published first September 18, 2019.

References

1. Garrido-Laguna I, Hidalgo M. Pancreatic cancer: from state-of-the-art treatments to promising novel therapies. Nat Rev Clin Oncol 2015;12:319–34.
2. Rahib L, Smith BD, Aizenberg R, Rosenzweig AB, Fleshman JM, Matrisian LM. Projecting cancer incidence and deaths to 2030: the unexpected burden of thyroid, liver, and pancreas cancers in the United States. Cancer Res 2014;74:2913–21.
3. American Cancer Society. Cancer Facts & Figures 2019. Atlanta: American Cancer Society; 2019.
4. Burris HA, 3rd, Moore MJ, Andersen J, Green MR, Rothenberg ML, Modiano MR, et al. Improvements in survival and clinical benefit with gemcitabine as first-line therapy for patients with advanced pancreas cancer: a randomized trial. J Clin Oncol 1997;15:2403–13.
5. Kim MP, Gallick GE. Gemcitabine resistance in pancreatic cancer: picking the key players. Clin Cancer Res 2008;14:1284–5.
6. Conroy T, Desseigne F, Ychou M, Bouche O, Guimbaud R, Becouarn Y, et al. FOLFIRINOX versus gemcitabine for metastatic pancreatic cancer. N Engl J Med 2011;364:1817–25.

Published OnlineFirst September 18, 2019; DOI: 10.1158/1078-0432.CCR-19-0799

7. Von Hoff DD, Ervin T, Arena FP, Chiorean EG, Infante J, Moore M, et al. Increased survival in pancreatic cancer with nab-paclitaxel plus gemcitabine. N Engl J Med 2013;369:1691–703.
8. Jia Y, Xie J. Promising molecular mechanisms responsible for gemcitabine resistance in cancer. Genes Dis 2015;2:299–306.
9. Jope RS, Yuskaitis CJ, Beurel E. Glycogen synthase kinase-3 (GSK3): inflammation, diseases, and therapeutics. Neurochem Res 2007;32: 577–95.
10. Doble BW, Woodgett JR. GSK-3: tricks of the trade for a multi-tasking kinase. J Cell Sci 2003;116(Pt 7):1175–86.
11. Ougolkov AV, Fernandez-Zapico ME, Bilim VN, Smyrk TC, Chari ST, Billadeau DD. Aberrant nuclear accumulation of glycogen synthase kinase-3beta in human pancreatic cancer: association with kinase activity and tumor dedifferentiation. Clin Cancer Res 2006;12:5074–81.
12. Ougolkov AV, Fernandez-Zapico ME, Savoy DN, Urrutia RA, Billadeau DD. Glycogen synthase kinase-3beta participates in nuclear factor kappaB-mediated gene transcription and cell survival in pancreatic cancer cells. Cancer Res 2005;65:2076–81.
13. Zhang JS, Koenig A, Harrison A, Ugolkov AV, Fernandez-Zapico ME, Couch FJ, et al. Mutant K-Ras increases GSK-3beta gene expression via an ETS-p300 transcriptional complex in pancreatic cancer. Oncogene 2011;30: 3705–15.
14. Garcea G, Manson MM, Neal CP, Pattenden CJ, Sutton CD, Dennison AR, et al. Glycogen synthase kinase-3 beta; a new target in pancreatic cancer? Curr Cancer Drug Targets 2007;7:209–15.
15. Mishra R. Glycogen synthase kinase 3 beta: can it be a target for oral cancer. Mol Cancer 2010;9:144.
16. Ding L, Liou GY, Schmitt DM, Storz P, Zhang JS, Billadeau DD. Glycogen synthase kinase-3beta ablation limits pancreatitis-induced acinar-to-ductal metaplasia. J Pathol 2017;243:65–77.
17. Kurosu T, Nagao T, Wu N, Oshikawa G, Miura O. Inhibition of the PI3K/Akt/GSK3 pathway downstream of BCR/ABL, Jak2-V617F, or FLT3-ITD downregulates DNA damage-induced Chk1 activation as well as G_2–M arrest and prominently enhances induction of apoptosis. PLoS One 2013; 8(11):e79478. doi: 10.1371/journal/pone.0079478.
18. Namba T, Kodama R, Moritomo S, Hoshino T, Mizushima T. Zidovudine, an anti-viral drug, resensitizes gemcitabine-resistant pancreatic cancer cells to gemcitabine by inhibition of the Akt-GSK3beta-Snail pathway. Cell Death Dis 2015;6:e1795.
19. Meijer L, Skaltsounis AL, Magiatis P, Polychronopoulos P, Knockaert M, Leost M, et al. GSK-3-selective inhibitors derived from Tyrian purple indirubins. Chem Biol 2003;10:1255–66.
20. Stambolic V, Ruel L, Woodgett JR. Lithium inhibits glycogen synthase kinase-3 activity and mimics wingless signalling in intact cells. Curr Biol 1996;6:1664–8.
21. Peng Z, Ji Z, Mei F, Lu M, Ou Y, Cheng X. Lithium inhibits tumorigenic potential of PDA cells through targeting hedgehog-GLI signaling pathway. PLoS One 2013;8:e61457.
22. Ban JO, Oh JH, Son SM, Won D, Song HS, Han SB, et al. Troglitazone, a PPAR agonist, inhibits human prostate cancer cell growth through inactivation of NFkappaB via suppression of GSK-3beta expression. Cancer Biol Ther 2011;12:288–96.
23. Shimasaki T, Ishigaki Y, Nakamura Y, Takata T, Nakaya N, Nakajima H, et al. Glycogen synthase kinase 3beta inhibition sensitizes pancreatic cancer cells to gemcitabine. J Gastroenterol 2012;47:321–33.
24. Mamaghani S, Patel S, Hedley DW. Glycogen synthase kinase-3 inhibition disrupts nuclear factor-kappaB activity in pancreatic cancer, but fails to sensitize to gemcitabine chemotherapy. BMC Cancer 2009;9:132.
25. Zamek-Gliszczynski MJ, Abraham TL, Alberts JJ, Kulanthaivel P, Jackson KA, Chow KH, et al. Pharmacokinetics, metabolism, and excretion of the glycogen synthase kinase-3 inhibitor LY2090314 in rats, dogs, and humans: a case study in rapid clearance by extensive metabolism with low circulating metabolite exposure. Drug Metab Dispos 2013;41: 714–26.
26. Gaisina IN, Gallier F, Ougolkov AV, Kim KH, Kurome T, Guo S, et al. From a natural product lead to the identification of potent and selective benzofuran-3-yl-(indol-3-yl)maleimides as glycogen synthase kinase 3beta inhibitors that suppress proliferation and survival of pancreatic cancer cells. J Med Chem 2009;52:1853–63.
27. Hilliard TS, Gaisina IN, Muehlbauer AG, Gaisin AM, Gallier F, Burdette JE. Glycogen synthase kinase 3beta inhibitors induce apoptosis in ovarian cancer cells and inhibit in-vivo tumor growth. Anticancer Drugs 2011;22: 978–85.
28. Sagar G, Sah RP, Javeed N, Dutta SK, Smyrk TC, Lau JS, et al. Pathogenesis of pancreatic cancer exosome-induced lipolysis in adipose tissue. Gut 2016; 65:1165–74.
29. Ugolkov A, Qiang W, Bondarenko G, Procissi D, Gaisina I, James CD, et al. Combination treatment with the GSK-3 inhibitor 9-ING-41 and CCNU cures orthotopic chemoresistant glioblastoma in patient-derived xenograft models. Transl Oncol 2017;10:669–78.
30. Zhang JS, Herreros-Villanueva M, Koenig A, Deng Z, de Narvajas AA, Gomez TS, et al. Differential activity of GSK-3 isoforms regulates NF-κB and TRAIL- or TNFalpha induced apoptosis in pancreatic cancer cells. Cell Death Dis 2014;5:e1142.
31. Ding L, Han L, Dube J, Billadeau DD. WASH regulates glucose homeostasis by facilitating Glut2 receptor recycling in pancreatic beta cells. Diabetes 2018;68:377–86.
32. Pal K, Cao Y, Gaisina IN, Bhattacharya S, Dutta SK, Wang E, et al. Inhibition of GSK-3 induces differentiation and impaired glucose metabolism in renal cancer. Mol Cancer Ther 2014;13:285–96.
33. Ugolkov A, Gaisina I, Zhang JS, Billadeau DD, White K, Kozikowski A, et al. GSK-3 inhibition overcomes chemoresistance in human breast cancer. Cancer Lett 2016;380:384–92.
34. Stephan S, Datta K, Wang E, Li J, Brekken RA, Parangi S, et al. Effect of rapamycin alone and in combination with antiangiogenesis therapy in an orthotopic model of human pancreatic cancer. Clin Cancer Res 2004;10: 6993–7000.
35. Tang J, Erikson RL, Liu X. Checkpoint kinase 1 (Chk1) is required for mitotic progression through negative regulation of polo-like kinase 1 (Plk1). Proc Natl Acad Sci U S A 2006;103:11964–9.
36. Cimprich KA, Cortez D. ATR: an essential regulator of genome integrity. Nat Rev Mol Cell Biol 2008;9:616–27.
37. Liu S, Bekker-Jensen S, Mailand N, Lukas C, Bartek J, Lukas J. Claspin operates downstream of TopBP1 to direct ATR signaling towards Chk1 activation. Mol Cell Biol 2006;26:6056–64.
38. Morishima K, Sakamoto S, Kobayashi J, Izumi H, Suda T, Matsumoto Y, et al. TopBP1 associates with NBS1 and is involved in homologous recombination repair. Biochem Biophys Res Commun 2007;362:872–9.
39. Jeon Y, Ko E, Lee KY, Ko MJ, Park SY, Kang J, et al. TopBP1 deficiency causes an early embryonic lethality and induces cellular senescence in primary cells. J Biol Chem 2011;286:5414–22.
40. Blackford AN, Patel RN, Forrester NA, Theil K, Groitl P, Stewart GS, et al. Adenovirus 12 E4orf6 inhibits ATR activation by promoting TOPBP1 degradation. Proc Natl Acad Sci U S A 2010;107:12251–6.
41. Walz A, Ugolkov A, Chandra S, Kozikowski A, Carneiro BA, O'Halloran TV, et al. Molecular pathways: revisiting glycogen synthase kinase-3beta as a target for the treatment of cancer. Clin Cancer Res 2017;23:1891–7.
42. Ugolkov AV, Matsangou M, Taxter TJ, O'Halloran TV, Cryns VL, Giles FJ, et al. Aberrant expression of glycogen synthase kinase-3beta in human breast and head and neck cancer. Oncol Lett 2018;16:6437–44.
43. Ugolkov AV, Bondarenko GI, Dubrovskyi O, Berbegall AP, Navarro S, Noguera R, et al. 9-ING-41, a small-molecule glycogen synthase kinase-3 inhibitor, is active in neuroblastoma. Anticancer Drugs 2018;29:717–24.
44. Zhou BB, Elledge SJ. The DNA damage response: putting checkpoints in perspective. Nature 2000;408:433–9.
45. Lecona E, Fernandez-Capetillo O. Targeting ATR in cancer. Nat Rev Cancer 2018;18:586–95.
46. Matsuoka S, Ballif BA, Smogorzewska A, McDonald ER 3rd, Hurov KE, Luo J, et al. ATM and ATR substrate analysis reveals extensive protein networks responsive to DNA damage. Science 2007;316:1160–6.
47. Karnitz LM, Flatten KS, Wagner JM, Loegering D, Hackbarth JS, Arlander SJ, et al. Gemcitabine-induced activation of checkpoint signaling pathways that affect tumor cell survival. Mol Pharmacol 2005;68:1636–44.
48. Koh SB, Courtin A, Boyce RJ, Boyle RG, Richards FM, Jodrell DI. CHK1 inhibition synergizes with gemcitabine initially by destabilizing the DNA Replication Apparatus. Cancer Res 2015;75:3583–95.
49. Wallez Y, Dunlop CR, Johnson TI, Koh SB, Fornari C, Yates JWT, et al. The ATR inhibitor AZD6738 synergizes with gemcitabine in vitro and in vivo to induce pancreatic ductal adenocarcinoma regression. Mol Cancer Ther 2018;17:1670–82.
50. Kumagai A, Lee J, Yoo HY, Dunphy WG. TopBP1 activates the ATR-ATRIP complex. Cell 2006;124:943–55.

AACR American Association for Cancer Research

Clinical Cancer Research

Glycogen Synthase Kinase-3 Inhibition Sensitizes Pancreatic Cancer Cells to Chemotherapy by Abrogating the TopBP1/ATR-Mediated DNA Damage Response

Li Ding, Vijay S. Madamsetty, Spencer Kiers, et al.

Clin Cancer Res Published OnlineFirst September 18, 2019.

Updated version Access the most recent version of this article at: doi:10.1158/1078-0432.CCR-19-0799